

Monte Carlo simulation of a grafted polymer chain confined in a tube

P. Sotta^{a)}

Laboratoire de Physique des Solides (CNRS UMR8502), Université Paris-Sud, Bât. 510,
91405 Orsay Cedex, France

A. Lesne and J. M. Victor

Laboratoire de Physique Théorique des Liquides, Université Pierre et Marie Curie, 4, Place Jussieu,
75252 Paris Cedex 05, France

(Received 27 July 1999; accepted 11 October 1999)

We study a grafted polymer chain confined in a tube by Monte Carlo simulations of a self-avoiding walk on a cubic lattice. We measure the probability distribution of the one-dimensional gyration radius r_{\parallel} and of the length of tube z occupied by the chain. We use a biased Monte Carlo algorithm in order to sample a large interval of r_{\parallel} or z . A simple scaling law is proposed for the length of tube z occupied by the chain, in the regime where the chain behaves as a linear, one-dimensional packing of units submitted to excluded-volume (blobs). A simple scaling law is also proposed for the number of contacts as a function of z . A model expression for the free energy of the confined chain is then deduced. It has a scaling structure similar to that of a free self-avoiding walk, with a different exponent of z in the small z regime. © 2000 American Institute of Physics.
[S0021-9606(00)50202-5]

I. INTRODUCTION

The problem of squeezing a polymer chain of length N monomers in a tube of diameter D is important for a number of reasons. Models to describe such a confined polymer chain, based on scaling arguments, have been developed long ago, for polymers in solution^{1,2} or in melts.³ Also, the structure of a semidilute solution confined in a porous medium has been observed recently by small angle neutron scattering.⁴

We consider here a closely related, but slightly different, problem. A self-avoiding chain is confined in a pore, and there is a perpendicular wall at some point in the pore, on which the chain is grafted at one end (Fig. 1). We consider this problem for two reasons. First, it may be related itself to some interesting physical situation or application (adhesion, friction, permeation of an actual isolated polymer through a pore or through a membrane). Then, we intend to extend it and use some of the results obtained here as a basis to understand the structure of grafted polymer brushes, their collapse in poor solvent or their stretched regime (as it is predicted for instance in grafted polyelectrolyte brushes.⁵⁻⁷)

The aim of the present work is to study the coil-globule transition for a neutral chain confined in a pore. The extension of the geometrical coil-globule transition of a free, isolated chain to a confined chain is not straightforward, since the geometry (and dimensionality) of the problem is quite different. In particular, there are two geometrical control parameters, the pore diameter D and the chain length N . Basic physical quantities relevant in this problem are the length of tube R_{\parallel} occupied by the chain, and the energy required to confine the grafted chain in it. We consider here a chain in

good solvent, i.e. described locally by the self-avoiding walk (SAW) statistics. R_{\parallel} must have the scaling form,²

$$R_{\parallel} = R_F \Phi(R_F/D). \quad (1)$$

R_F is the Flory gyration radius of a real chain in good solvent, which scales as $R_F \approx aN^{\nu}$, with $\nu = 3/5$ in 3 dimensions and a is the monomer length.

Since there is no confinement in a thick tube, the function Φ has to meet the requirement $\Phi \rightarrow 1$ when the ratio $x = R_F/D \rightarrow 0$. In the strong confinement limit $x \rightarrow \infty$ (thin tube), a scaling law $\Phi(x) \approx x^m$ is assumed, m is determined by the condition that R_{\parallel} be a linear function of N for strong confinement, because the problem is then one-dimensional. For $a \ll D \ll R_F$, this leads to the following scaling:

$$R_{\parallel} \approx aN \left(\frac{a}{D} \right)^{2/3}. \quad (2)$$

As soon as $D \ll aN^{3/5}$, the chain is extended along the tube, $R_{\parallel} \gg R_F$. The concentration inside the chain is independent of N ,

$$c \approx \frac{N}{D^2 R_{\parallel}} \approx a^{-3} \left(\frac{a}{D} \right)^{4/3}. \quad (3)$$

The above considerations may be interpreted in terms of a ‘blob’ picture. In a semidilute solution in good solvent, a blob is a region of space occupied by a portion of a single chain. Inside each blob, excluded volume interactions between monomers are *not* screened, and the corresponding portion of chain obeys the Flory statistics. Thus, the number of monomers per blob g is given by $ag^{3/5} = D$. Equation (2) is then obtained by packing a sequence of N/g blobs linearly along the tube.

Finally, the elastic free energy of the chain confined in the pore is estimated as

^{a)} Author to whom correspondence should be addressed; electronic mail: sotta@lps.u-psud.fr

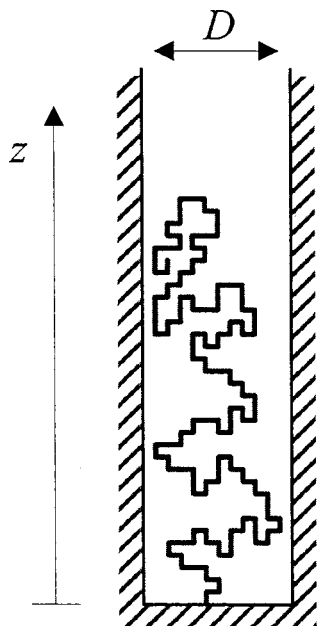


FIG. 1. Schematics of the grafted linear chain confined in a pore, simulated on a cubic lattice.

$$F_{\text{conf}} \approx k_B T N \left(\frac{a}{D} \right)^{5/3}. \quad (4)$$

This corresponds to attributing a free energy $k_B T$ per blob. Equation (4) is the same as for a free chain in the limit of large elongation.

Scaling predictions, Eqs. (2) and (3), have been established on a firm basis in grafted polymers and brushes.^{8,9} We investigate here the statistics of the length (or gyration radius) r_{\parallel} occupied in a tube by a linear self-avoiding chain squeezed in it. The equilibrium quantity R_{\parallel} mentioned above is simply the thermal average of this length. Our approach relies on a geometrical (“blob”) model describing the structure of the chain, substantiated both with previously obtained distributions of the radius of gyration of a SAW,^{10–14} and Monte Carlo simulations.

The paper is organized as follows. In Sec. II, we present a model for the distribution of the length r occupied by a chain confined in a tube. This is a straightforward extension of the previously obtained distribution for the gyration radius of a SAW. We conjecture also an expression for the number of contacts, i.e., the energy, in such a chain. Technicalities of the Monte Carlo simulations are presented in Sec. III. Results are presented in Sec. IV. Numerical, scaling expressions are proposed for the number of configurations and the number of contacts as a function of the length r . From these expressions, an expression for the free energy may be deduced, as it is presented in Sec. V.

II. MODEL

A. Scaling form for the gyration radius distribution

The approach in terms of a distribution for the gyration radius of a polymer chain has been initiated long ago. First,

the distribution for the gyration radius r of a linear polymer was established to be (only r -dependent terms are retained) in d dimensions,¹⁰

$$\ln P(r) \approx -N \left[\left(\frac{Na^3}{r^3} \right)^{\alpha} + \left(\frac{r}{Na} \right)^{\delta} \right], \quad (5)$$

where $\alpha = 1/(\nu d - 1) = 5/4$ and $\delta = 1/(1 - \nu) = 5/2$ (we shall consider the case $d=3$ in all what follows). Equation (5) expresses the probability $P(r)$ to obtain an instantaneous value r for the gyration radius of the polymer [$P(r)$ is proportional to the number of configurations giving a gyration radius r]. It was established on the basis of scaling considerations, within a phenomenological approach, and tested numerically for chains generated on a square lattice.^{10–12,15} Then, for a chain squeezed in a tube of diameter D , the characteristic length to be considered is the one-dimensional gyration radius (measured along the tube) r_{\parallel} . Equation (5) becomes¹⁰

$$\ln P(r_{\parallel}) \approx -N \left[\left(\frac{Na^3}{r_{\parallel} D^2} \right)^{\alpha} + \left(\frac{r_{\parallel}}{Na} \right)^{\delta} \right]. \quad (6)$$

The second term on the right-hand side describes the stretched regime. It corresponds to values of r_{\parallel} such that the chain is more stretched than due to the confinement in the pore. Thus, the statistics becomes independent of the pore diameter in this regime. The first term describes the collapsed regime, in which the number of configurations is a function of the concentration inside the tube $c = N/r_{\parallel} D^2$ only. Equation (6) may be rewritten in the scaling form,

$$\ln P(r_{\parallel}) \approx -N \left(\frac{D}{a} \right)^{-5/3} [x^{-5/4} + x^{5/2}]. \quad (7)$$

$x = r_{\parallel}/r_m$ is the (one-dimensional) reduced gyration radius, with $r_m = Na(D/a)^{-2/3}$ the equilibrium elongation of the chain, obtained as the r_{\parallel} value corresponding to the maximum of the distribution $P(r_{\parallel})$. Note that the exponent $-2/3$ is *not* trivial. It is directly related to the Flory exponent ν_F . It reflects the fact that there is an excluded volume (Flory) behavior at small spatial scales and a screened behavior at larger scales, with a crossover in between the two regimes. The crossover occurs at a certain correlation length, and the blob concept is based on this correlation length.

The linear relation $r_m \approx N$ may not hold in the intermediate regime in which r_{\parallel} is comparable to D . In this case, which corresponds to weak confinement, the number of blobs is essentially equal to one.

The power law at large r_{\parallel} values is the same for a free and confined polymer [Eqs. (5) and (6)]. This corresponds to a linearly stretched polymer. In this regime, the polymer may be described as a linear packing of blobs of size ξ , with $g = (\xi/a)^{1/\nu}$ monomers per blob, leading to the following relation between the size r_{\parallel} of the polymer and its lateral dimension ξ , $r_{\parallel} = Na^{1/\nu} \xi^{1-1/\nu}$. By comparing the lateral size ξ to the pore diameter D , one finds the crossover to the r_{\parallel} -regime in which the polymer becomes insensitive to the pore confinement. This condition is $r_{\parallel} \geq Na(D/a)^{-2/3} \equiv r_m$. Thus, the same behavior as that of a free polymer would be expected in the whole domain $r_{\parallel} \geq r_m$.

Note finally that, for a linearly stretched polymer, which is a one-dimensional system, it is equivalent to consider the one-dimensional gyration radius r_{\parallel} or the (linearly) averaged length z . Both quantities are expected to be proportional.

B. Logarithmic corrections

As a consequence of its unidimensional confinement, the chain behaves as a succession of statistically independent subunits (“blobs”), whose size is fixed by the pore diameter. We look for the total number of configurations $\Omega_{N,D}(r)$ of an N -chain which has a characteristic length r_{\parallel} along the tube (this length being measured either by the one-dimensional gyration radius r_{\parallel} or by the average length z). The chain is a succession of $B=N/g$ statistically independent blobs (note that B depends on z). Then,

$$\Omega_{N,D}(r_{\parallel}) = [\Omega_g(D)]^{N/g} = [\mu^g g^{\gamma-1} P_g(D)]^{N/g} = \mu^N g^{(\gamma-1)N/g} e^{-N[(g a^3/D^3)^{\alpha} + (D/g a)^{\delta}]} \tag{8}$$

The occupied length r_{\parallel} is $r_{\parallel} = DB = DN/g$. This gives the complete form of Eq. (6),

$$\ln \Omega_{N,D}(r_{\parallel}) \approx (1-\gamma) \frac{r_{\parallel}}{D} \ln \frac{r_{\parallel}}{ND} - N \left[\left(\frac{Na^3}{r_{\parallel} D^2} \right)^{\alpha} + \left(\frac{r_{\parallel}}{Na} \right)^{\delta} \right], \tag{9}$$

which may be rewritten,

$$\begin{aligned} \ln \Omega_{N,D}(r_{\parallel}) &\approx \ln P_{N,D}(r_{\parallel}) \\ &\approx -N \left(\frac{D}{a} \right)^{-5/3} \left[(\gamma-1)x \ln x \right. \\ &\quad \left. - \frac{5}{3} (\gamma-1)x \ln \frac{D}{a} + x^{-5/4} + x^{5/2} \right], \end{aligned} \tag{10}$$

with $x = (r_{\parallel}/r_m) = (r_{\parallel}/Na)(D/a)^{2/3}$ as before. Hence, logarithmic corrections to Eq. (7) appear in Eq. (10). For a given value of the pore diameter D , the scaling form $\ln P_{N,D}(r_{\parallel})/ND^{-5/3} = f(x)$ is retained. In three dimensions, the universal exponent $\gamma-1 \cong 1/6$.² The terms $x^{-5/4}$ and $x^{5/2}$ are only the first, dominant terms of a series expansion, and the right-hand side of Eq. (10) should also contain power-law terms of higher order. These will be discussed later. The chain here is supposed to be uniformly stretched (or squeezed), i.e., the density is the same in all the blobs. This means that a saddle point approximation is done; for a given total elongation r_{\parallel} , the chain is supposed to acquire a conformation with the same average density in each blob. Thus, configurations with nonequivalent blobs are supposed to have a negligible statistical weight. This argument is no longer relevant in the stretched regime (large z or r_{\parallel} values), in which different blobs are *not* independent. However, in this regime, the statistics is independent of the blob diameter, and scaling terms of the form $r_{\parallel}/N^{5/2}$ (and higher order terms) are retained only. A first part of this work shall consist in testing the scaling prediction Eq. (7) and examining whether logarithmic corrections may be measured.

C. The number of contacts in a polymer chain confined in a pore

The number of contacts in a SAW with a gyration radius r obeys the scaling law,¹²

$$m_N(r) \approx aN1 + \left(\frac{N}{r^d} \right)^{\alpha} - \frac{r}{N}^{\delta}, \tag{11}$$

with $\alpha = (\nu d - 1)^{-1} = 5/4$ and $\delta = (1 - \nu)^{-1} = 5/2$. Equation (11) may be written equivalently $m_N(r) - aN \approx (R_F/r)^{d/(\nu d - 1)} - (r/R_F)^{1/(1 - \nu)}$ with $R_F = aN^{\nu}$. Within the blob picture described above, the average number of contacts within a blob of size g is

$$m_g(D) \approx ag \left[1 + \left(\frac{g}{D^d} \right)^{1/(\nu d - 1)} - \left(\frac{D}{g} \right)^{1/(1 - \nu)} \right]. \tag{12}$$

Note that this is the *total* number of contacts in the blob, not the average number of contact *per monomer*. The number of blobs per chain is N/g , and $g \approx ND/z$. Thus, from Eq. (12), the total number of contacts in the chain is finally, for $d=3$ and $\nu=3/5$,

$$m_{D,N}(r_{\parallel}) \approx N \left[1 + D^{-5/3} x^{-5/4} - D^{-5/3} x^{5/2} \right] \tag{13}$$

in which x is the (one-dimensional) reduced gyration radius, as in Eqs. (7) and (10). The second term corresponds to the compact side and the third one to the stretched side. Contacts between different blobs have been neglected. It was shown in Ref. 12 that a surface term has to be introduced in Eq. (13) to reproduce simulated results, for a free (isolated) SAW. The situation here is different, even though the surface-to-volume ratio of the confined polymer is higher than for a free polymer, since both the volume and surface are linear in the chain length N . Thus, the effect of the surface is simply to multiply the number of contacts by a constant amount (independent of x), of the order $1 - 1/D$.

III. TECHNICALITIES OF THE SIMULATIONS

Three-dimensional self-avoiding walks of length N sites are generated on a square lattice, using a Monte Carlo method. The chain is both grafted and confined in a pore (see Fig. 1). The pore has a square section of surface area $S = D^2$. The grafting surface and the pore are defined by unpenetrable walls. Unit moves used to generate chain configurations are free extremity rotations, L -inversions and kink-shifts.^{16,17} There is no bending energy. Different chain lengths ($N=150-400$) and different pore sizes ($D=5-9$) were investigated. In each simulation, typically $10^7-2 \times 10^7$ MC steps were performed (one MC step is a cycle of N attempted elementary moves). The system was equilibrated during a typical time $\tau \cong 0.25N^2$ MC steps before starting the measurements.^{8,18} The free, grafted chain of length $N=150-300$ was placed in a box of lateral dimensions $2\sqrt{N}$ with periodic boundary conditions on the lateral walls.

Two quantities were measured:

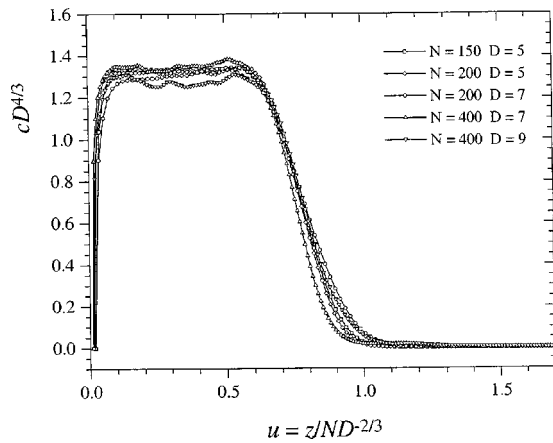


FIG. 2. The reduced density $cD^{4/3}$ as a function of the reduced distance to the grafting surface $Z/ND^{-2/3}$ (here Z denotes the distance to the surface).

- (1) The one-dimensional gyration radius along the pore direction, given by

$$r_{\parallel} = \left[\frac{1}{2N^2} \sum_{i=1}^N \sum_{j=1}^N (z_i - z_j)^2 \right]^{1/2}. \quad (14)$$

- (2) The average length of the chain above the grafting surface, given by

$$z = \frac{1}{N} \sum_{i=1}^N z_i. \quad (15)$$

The distributions $P_{N,D}(r_{\parallel})$ and $P_{N,D}(z)$ were accumulated during the simulations. Typically, r and z were measured 10^6 – 4×10^6 times. The average concentration profile $d(Z)$ along the pore direction was measured additionally (here Z denotes the distance to the grafting surface). The concentration profiles for different values of N and D are shown in Fig. 2. The concentration is uniform over quite a large Z interval, as expected (see Sec. II). Also, in Fig. 2, the profiles are normalized to show the scaling behavior of the concentration, according to Eq. (3).

In a second series of simulations, two-dimensional joint distributions $P_{N,D}(r_{\parallel}, m)$ and $P_{N,D}(z, m)$ were measured; $P_{N,D}(z, m)$ [or similarly $P_{N,D}(r_{\parallel}, m)$] give the number of configurations with a given length z (or r_{\parallel}) and a given number of contacts m . The distribution $P_{N,D}(z)$ [or $P_{N,D}(r_{\parallel})$] is recovered as

$$P_{N,D}(z) = \sum_m P_{N,D}(z, m). \quad (16)$$

The number of contacts as a function of z (or r) is given by

$$m_{N,D}(z) = \frac{\sum_m m P_{N,D}(z, m)}{\sum_m P_{N,D}(z, m)}. \quad (17)$$

The average number of contacts $\langle m_{N,D} \rangle$ is determined by

$$\langle m_{N,D} \rangle = \frac{\sum_z m_{N,D}(z) P_{N,D}(z)}{\sum_z P_{N,D}(z)}. \quad (18)$$

z should theoretically range from $z_{\min} \approx Na(D/a)^{-2}$ to $z_{\max} \approx Na$. In practice, the simulated values range in a much narrower interval around z_0 , from $z_0/2$ to $2z_0$ typically. In order to get a large number of configurations in a wide interval of the parameter z (or equivalently, r_{\parallel}), we biased the Monte Carlo algorithm with an effective Boltzmann factor of the form e^{Kz} , where K is an adjustable statistical weight. As a result, for each K value, a partial histogram $P_{N,D,K}(z, m) = P_{N,D}(z, m)e^{Kz}$ is obtained, where $P_{N,D}(z, m)$ is the unbiased distribution, sampled in a z -interval which depends itself on K . The major advantage of the technique is that the statistical weight $P_{N,D}(z, m)$ in this K -dependent z -interval would be impossible to measure in an unbiased simulation. The enlarged distribution $P_{N,D}(z, m)$ is obtained by merging together the histograms $P_{N,D,K}(z, m)$ obtained with different values of K , according to a well documented procedure.^{13,19} Simulations with positive (resp. negative) values of K sample large (resp. small) values of z and r_{\parallel} . Note that the number of contacts $m_{N,D,K}(z)$ [or $m_{N,D,K}(r_{\parallel})$] obtained with a statistical weight K does not depend on K [see Eq. (18)], only the z -interval (or r_{\parallel} -interval) does. Thus, in a series of simulations with different statistical weights K , the whole function $m_{N,D}(r_{\parallel})$ is computed directly as

$$m_{N,D}(r_{\parallel}) = \frac{\sum_k P_{N,D,K}(r_{\parallel}) m_{N,D,K}(r_{\parallel})}{\sum_k P_{N,D,K}(r_{\parallel})}. \quad (19)$$

In practice, 8–16 different K values, ranging from -4 to $+4$ typically, were used in each simulation. Note that another advantage of this procedure is that simulations with different K values may be run in parallel.

IV. RESULTS

A. Scaling law for the gyration radius

r_{\parallel} is the one-dimensional gyration radius as defined in Eq. (14). The reduced gyration radius is defined here as $\rho = r_{\parallel}/ND^{-2/3}$ (r_m is the most probable r_{\parallel} value, i.e., the value at the maximum of the distribution). Neglecting the influence of the logarithmic term in Eq. (10), one expects the quantity $G(\rho)/ND^{-5/3} = \ln(P(r_{\parallel})/P(r_m))/ND^{-5/3}$ to be a universal function of the reduced gyration radius. In Fig. 3 the curves $G(\rho)/ND^{-5/3}$ are plotted as a function of ρ , for different values of N and D . Within experimental uncertainties, all curves collapse on a unique master curve. This result demonstrates the validity of the scaling law in Eq. (7), i.e., the universal behavior of the distribution $P(r_{\parallel})$. Note that no statistical weighting was applied here, so that only a small ρ interval is sampled.

Figure 4 shows the radius of gyration r_m corresponding to the maximum of the distribution $P(r_{\parallel})$, i.e., the most probable r_{\parallel} value. The quantity $r_m D^{2/3}$ is plotted as a function of N , for different values of N and D . The scaling law, Eq. (2), is verified. A linear fit of the data in Fig. 3 gives

$$r_m = bND^{-2/3} \quad (20)$$

with a prefactor $b = 0.22 \pm 0.005$, which, compared to Eq. (2), would correspond to an effective monomer size $a = b^{3/5} = 0.40314$. This value may be compared to that obtained for free, isolated SAW in 2D simulations ($b = 0.348 \pm 0.002$)

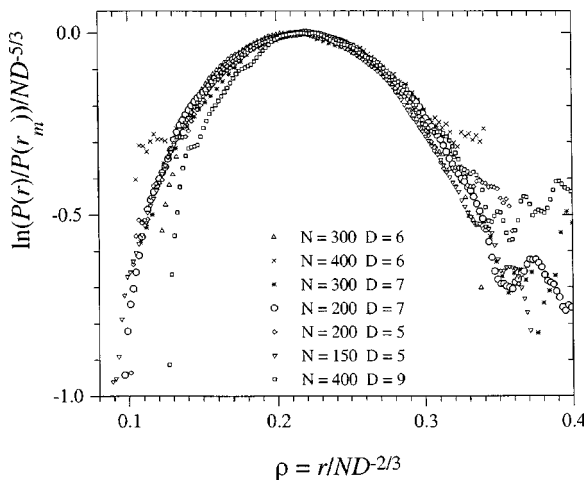


FIG. 3. The distribution $G(\rho) = \ln(P(r_{\parallel})/P(r_m))/ND^{-5/3}$ plotted as a function of the reduced gyration radius $\rho = r_{\parallel}/ND^{-2/3}$, for different values of N and D . All curves collapse on a unique master curve, which demonstrates the universal behavior of the distribution $P(r_{\parallel})$.

(Ref. 11) or in 3D simulations using a pivot algorithm¹⁶ (there, however, the gyration radius as a function of N was not measured explicitly). In Ref. 20, the value $a = 0.396$ was measured in a 3D SAW. Thus, our value agrees within 2% accuracy to that latter one. This value leads to an unperturbed gyration radius $R_F \approx 8$ (for $N = 150$) to $R_F \approx 14.6$ (for $N = 400$), which is typically 1.5 time larger than the largest pore diameter D studied here, for each value of N .

B. Scaling law for the average length of the chain

In the same way as above, the distributions $P(z)$ for the average length z [defined in Eq. (15)] were measured. In Fig. 5, the quantity $G(u)/ND^{-5/3} = \ln(P(z)/P(z_m))/ND^{-5/3}$ is plotted as a function of the reduced length $u = z/ND^{-2/3}$, for different values of N and D . All curves collapse on a unique master curve, which demonstrates that the scaling law in Eq. (7) is verified by the distribution $P(z)$ as well. On the other hand, it suggests that the influence of the logarithmic term is

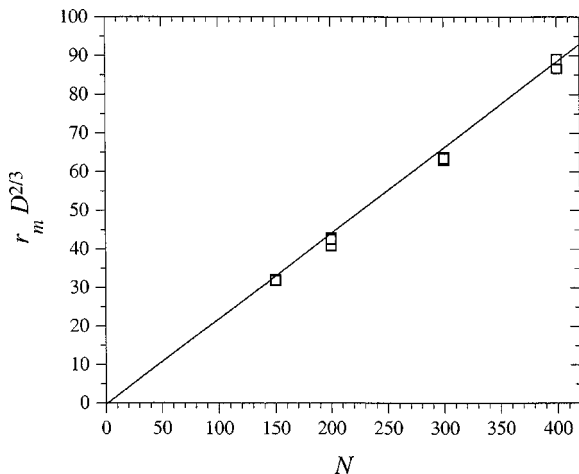


FIG. 4. The quantity $r_m D^{2/3}$ plotted as a function of N , for different values of N and D . r_m is the gyration radius corresponding to the maximum of the distribution $P(r_{\parallel})$.

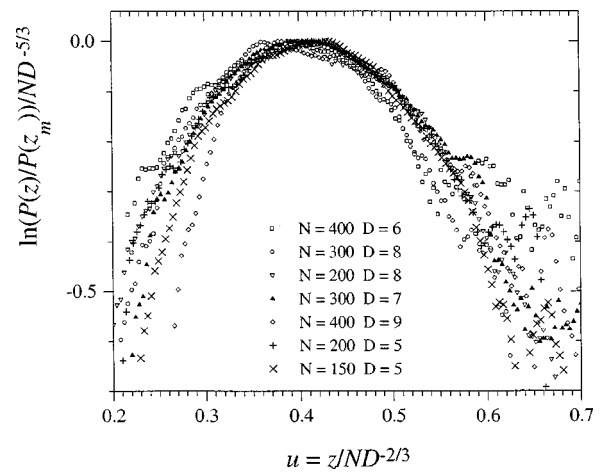


FIG. 5. The distribution $G(u) = \ln(P(z)/P(z_m))/ND^{-5/3}$ plotted as a function of the reduced length $u = z/ND^{-2/3}$, for different values of N and D . All curves collapse on a unique master curve, which demonstrates the universal behavior of the distribution $P(z)$.

rather weak. The average length z_m corresponding to the maximum of the distribution $P(z)$ was measured for the different values of N and D . We find

$$z_m = b' ND^{-2/3}. \tag{21}$$

The prefactor $b' = 0.4 \pm 0.01$, which would correspond to an effective monomer size $a = b'^{3/5} = 0.577$.

Thus, it has been shown that the distributions for both quantities r_{\parallel} and z have the same universal behavior, described by Eq. (7). This reflects essentially the one-dimensional behavior of the confined chain, in the limit $R_F \gg D$, i.e., the fact that the chain is essentially a collection of statistically independent blobs for all densities, i.e., throughout the distribution. This behavior is evidenced as well by the scaling of the density, as it was shown in Fig. 2. It is important to notice that the one-dimensional character of the chain statistics is established for values of the ratio R_F/D as low as 1.5.

However, it is clear that only very limited ranges of r_{\parallel} or z are sampled in Figs. 3 and 5. The range of u which is sampled in Fig. 5 is typically $0.3 \leq u \leq 0.55$. For example, for $D = 5$, the theoretically accessible u values range from $u_{\min} = D^{-4/3}/2 = 0.0585$ to $u_{\max} = D^{2/3}/2 = 1.462$. It is therefore necessary to bias the simulations to explore a significant part of the configurational space.

In the following, we apply a statistical weight (effective Boltzmann factor) of the form \exp^{Kz} (see Sec. III) and we use the distribution $P_{N,D}(z)$ to characterize the statistical properties of the chain. In Fig. 6, the curves $G(u)/ND^{-5/3}$ are plotted as a function of u , for different values of N and D . Here, each curve has been obtained on an enlarged u interval by merging together the distributions obtained with different values of the parameter K . All curves collapse on a unique master curve to a very good approximation. This result demonstrates the universal behavior of the distribution $P_{N,D}(z)$ [Eq. (7)]. The interval obtained in Fig. 6 is $0.11 < u < 1.3$, which is very close to the theoretical interval.

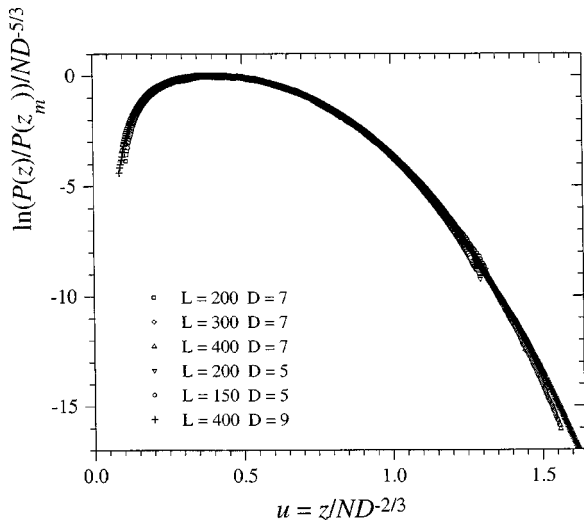


FIG. 6. Curves $G(u)$ obtained for different values of N and D (same as in Fig. 5). Here the curves $G(u)$ have been obtained by merging together histograms obtained with statistical weights of the form e^{Kz} . Thus the curves span a much larger z interval than in Fig. 5.

C. Fit of the distribution $P_{N,D}(z)$

In the stretched regime, finite size effects may come into play. The term corresponding to the large z regime in Eq. (7) is the first term of a series expansion in terms of z/Na , which writes $\ln P(z) \approx M[(z/Na)^{5/2} + (z/Na)^5 + \dots]$. In terms of the new variable $t = (z/N)^{5/2}$, this gives the following expansion:

$$h(t) \equiv \frac{\ln P_{N,D}(z)}{N} \cong h_{\text{small}}(t) + A_2 t + A_3 t^2. \quad (22)$$

$h_{\text{small}}(t)$ describes the behavior at small t values (i.e., at small z values) and verifies $h_{\text{small}}(t) \rightarrow 0$ when t is large. A higher order term A_3 has been introduced. In Fig. 7 the quantity $h(t)/t$ is plotted as a function of t . The different histograms have been normalized so that all curves $h(t)/t$ coin-

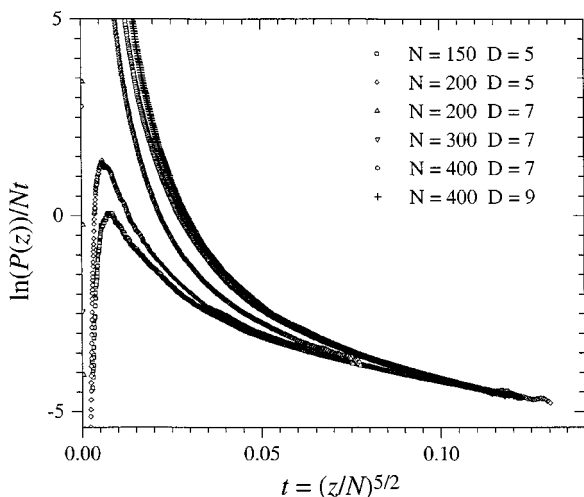


FIG. 7. The quantity $h(t)/t = \ln(P(z)/P(z_m))/Nt$ as a function of the variable $t = (z/N)^{5/2}$, for different values of N and D . The curves tend to a linear behavior at large t , with the same slope for all curves, which is in agreement with Eq. (22) in the text.

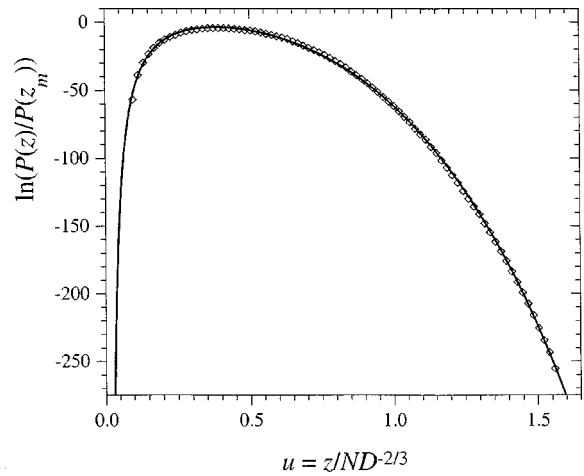


FIG. 8. The curve $G(u)$ obtained for $N=400$ and $D=7$ (same as in Fig. 6). The continuous curve is a fit to an equation of the form $g(u) = P_1 + P_2 u^{-5/4} + P_3 u^{5/2} + P_4 u^5$ [see Eq. (23) in Sec. IV C]. An excellent fit is obtained in the whole range of obtained u values.

cide at large t values. It is clear from Fig. 7 that $h(t)/t$ tends to a linear behavior at large t (large z) with a roughly constant limiting slope, which gives $A_3 = -17.73 \pm 1.4$. This shows that an additional power term has to be introduced to fit the distribution $P_{N,D}(z)$ at large z values, and that this term is of the expected form $N(z/Na)^5$.

The curves $G(u) = \ln(P(z)/P(z_m))$ were fitted to a function of the form $g(u) = P_1 + P_2 u^{-5/4} + P_3 u^{5/2} + P_4 u^5$. The fitting was done for different values of N and D , using the enlarged distributions $P_{N,D}(z)$ obtained in series of biased simulations. An example of the obtained fit is shown in Fig. 8. The results of the fits are summarized in Table I. For each of the curves, the agreement between theory and simulation is excellent. It is not possible to isolate and estimate logarithmic corrections in a satisfactory way. Indeed, both the fact that the fit is excellent for each curve and that curves obey the scaling behavior [Eq. (7)] to a very good approximation, indicates that logarithmic terms are only very small corrections to the scaling behavior and can be neglected here. In contrast, the higher order term u^5 cannot be ignored.

From the values in Table I, we may finally propose the following approximate form:

$$G(u)/ND^{-5/2} \cong -0.257u^{-5/4} - 4.03u^{5/2} - 13D^{-5/3}u^5, \quad (23)$$

TABLE I. The reduced histograms (see Figs. 6 and 8) $G(u)/ND^{-5/2} = \ln(P(u)/P(u_m))/ND^{-5/2}$ as a function of $u = z/ND^{-2/3}$ were fitted to a function of the form $g(u) = P_1 + P_2 u^{-5/4} + P_3 u^{5/2} + P_4 D^{-5/3} u^5$.

Chain length N	Pore diameter D	P_2	P_3	P_4
150	5	-0.277	-3.83	-11.32
200	5	-0.246	-3.77	-12.31
200	7	-0.278	-3.81	-16.96
300	7	-0.242	-4.10	-13.87
400	7	-0.232	-4.09	-12.94
400	9	-0.269	-4.57	-10.5

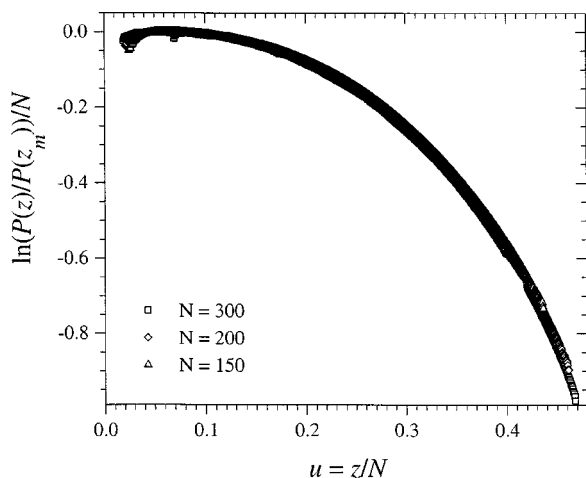


FIG. 9. The distribution $G(u) = \ln(P(z)/P(z_m))/N$ plotted as a function of the reduced length $u = z/N$, for isolated, grafted chains of different lengths N . The curves are obtained by merging histograms with different (positive) values of K . Only the part $z \geq z_m$ is drawn. All curves collapse on a unique master curve, which demonstrates the universal behavior of the distribution $P(z)$.

or equivalently, $G(u)/ND^{-5/3} \cong -0.808(u/u_m)^{-5/4} - 0.408(u/u_m)^{5/2} - 0.133D^{-5/3}(u/u_m)^5$, in which u_m is the u value at the maximum of the distribution [according to Eq. (21), $u_m = 0.4$].

D. Comparison to free, grafted chains

At high elongation, the distribution for a polymer in a pore is expected to coincide with that of a free polymer (see Sec. II A). Thus, simulations were done for a polymer chain grafted on a flat surface, without lateral walls. The quantity $\ln(P(z))/N$ is plotted as a function of $u = z/N$ in Fig. 9, for free chains of length $N = 150$ – 300 . Each curve has been obtained on a large u interval by merging together the distributions obtained with different positive values of the parameter K . Thus, only the part of the distribution on the right of the maximum (i.e., the part $z \geq z_m$) has been obtained here and is plotted in Fig. 9. All three curves collapse on a unique master curve to a very good approximation. This result shows that the terms with a positive power of z/N [see Eq. (6)] are predominant in the whole range $z \geq z_m$, leading to a practically universal behavior of the distribution $P(z)$ in all this interval of z values.

The quantity $h(t)$ as defined in Eq. (22), is plotted vs $t = (z/N)^{5/2}$ in Fig. 10 for free chains of length $N = 150$ – 300 . In this case as well, $h(t)$ tends to a linear behavior at large t values, with a slope A_3 comparable to the one obtained previously, $A_3 \cong -16.33$. The curve for a chain confined in a pore ($N = 200, D = 5$) is shown for comparison. Both curves have a linear asymptotic behavior with the same slope A_3 . On the other hand, the point at which the curves deviate from one another depends on the pore diameter D .

E. The number of contacts

The numbers of contacts $m_{N,D}(z)$ and $m_{N,D}(r_{\parallel})$ were obtained from 2D histograms giving the joint probability distributions $P_{N,D}(m, z)$ or $P_{N,D}(m, r_{\parallel})$, according to the proce-

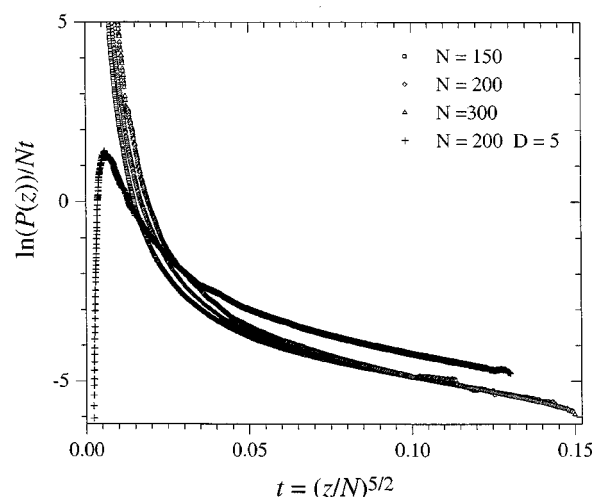


FIG. 10. The quantity $h(t) = \ln(P(z)/P(z_m))/Nt$ as a function of the variable $t = (z/N)^{5/2}$, for isolated, grafted chains of different lengths N . The curves superpose at large t , which is in agreement to Eq. (22) in the text. The curve $h(t)$ for a chain confined in a pore ($N = 200, D = 5$) is shown for comparison.

cedure described in Eqs. (17) and (19). Large z and r_{\parallel} intervals were sampled using series of biased simulations. The uncertainties in these curves is of the order one contact. The average numbers of contacts $\langle m_{N,D} \rangle$ were determined following Eq. (18). The values obtained for $\langle m_{N,D} \rangle$ and the average number of contacts $\bar{m}_{N,D} \equiv m_{N,D}(z_m)$ corresponding to the value z_m at the maximum of the distribution $P(z)$ are summarized in Table II. Both values $\langle m_{N,D} \rangle$ and $\bar{m}_{N,D}$ coincide to an excellent approximation. In agreement with Eq. (13), the ratio $\langle m_{N,D} \rangle/N$ (which is the average number is contacts per monomer) is constant, within experimental uncertainties. In particular, the number of contacts is independent of the pore diameter. Then, the quantity $(m_{N,D}(u) - \langle m_{N,D} \rangle)/ND^{-5/3}$ should be a universal function of $u = z/ND^{-2/3}$. This quantity is shown in Fig. 11 for different values of N and D . A universal curve is obtained at small u and in a large interval around $u = u_m$. This demonstrates the scaling behavior expressed in Eq. (13). At large values of u , $m_{N,D}(u)$ is expected to tend to zero contact and therefore to deviate from the behavior in Eq. (13). The curves $m_{N,D}(u)$ were fitted to a function of the form $f(u) = P_1 + P_2u^{-5/4} + P_3u^{5/2}$, in the domain $z \leq z_m$. Very good fits are obtained in the whole range, in which curves superpose. An example of fitting function is shown in Fig. 11. In contrast to free chains in good solvent, no surface term needs to be introduced here, due to the par-

TABLE II. The average numbers of contacts $\langle m_{N,D} \rangle$ have been computed according to Eq. (18). \bar{m} is the number of contacts $m(z_m)$ corresponding to the maximum z_m of the distribution $P_{N,D}(z)$.

Chain length N	Pore diameter D	$\langle m \rangle/N$	\bar{m}/N
150	5	0.2736	0.2727
200	5	0.2714	0.2749
200	7	0.2612	0.2598
300	7	0.2572	0.2617
400	7	0.2637	0.2646
400	9	0.2435	0.2512

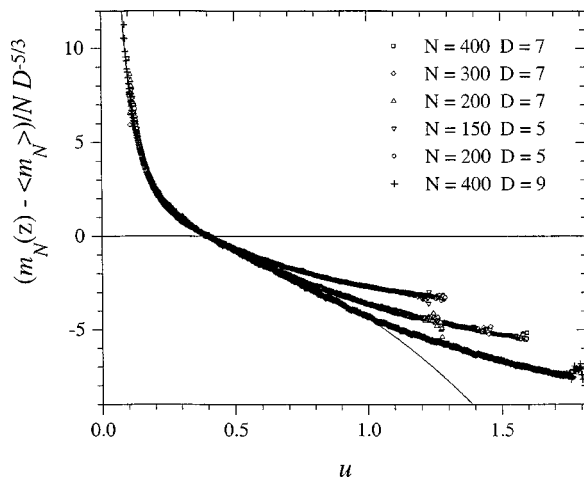


FIG. 11. The reduced number of contacts $(m - \langle m \rangle)/ND^{-5/3}$ as a function of $u = z/ND^{-2/3}$, for different values of N and D . The continuous curve is a fit to Eq. (13), in the domain $u \leq u_m$. All curves collapse on a unique master curve for $u \leq u_m$.

ticular geometry of this problem, as mentioned in Sec. II C. The influence of the surface is limited here to the extremity of the chain and is negligible. Finally, the following scaling form may be proposed:

$$\frac{m_{N,D}(u) - \langle m_{N,D} \rangle}{ND^{-5/3}} \cong -1.3 + 0.54u^{-5/4} - 3.6u^{5/2} \quad (24)$$

or equivalently $(m_{N,D}(u) - \langle m_{N,D} \rangle)/ND^{-5/3} \cong -1.3 + 1.65(u/u_m)^{-5/4} - 0.35(u/u_m)^{5/2}$.

Note that the coefficient P_2 may be estimated theoretically. For a completely collapsed chain, the length is $z_{\min} \approx N/D^2$, thus $u_{\min}/u_m = D^{-4/3}$, and the number of contacts per monomer is of the order 2, which, in the limit $N \rightarrow \infty$, leads to $P_2 \cong 2 - 0.26 = 1.74$ (with $\langle m_{N,D} \rangle \cong 0.26$). This is roughly comparable to the value 1.65 above.

In Fig. 12, the quantity $(m_{N,D}(r_{\parallel}) - \langle m_{N,D} \rangle)/ND^{-5/3}$ is plotted as a function of the reduced gyration radius $\rho = r_{\parallel}/ND^{-5/3}$ for different values of N and D . The scaling

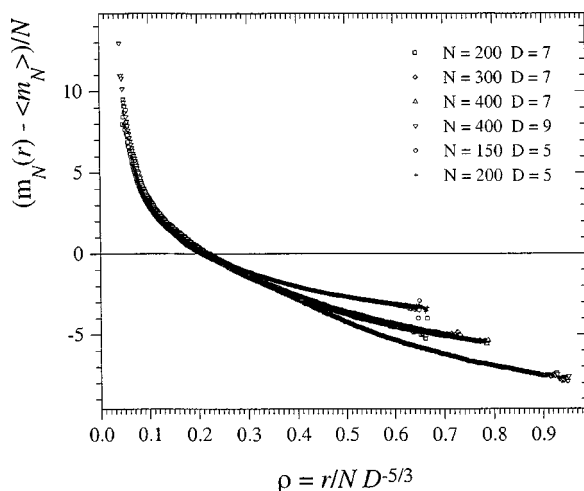


FIG. 12. The reduced number of contacts $(m - \langle m \rangle)/ND^{-5/3}$ as a function of $\rho = r_{\parallel}/ND^{-5/3}$, for different values of N and D . All curves collapse on a unique master curve for $u \leq u_m$.

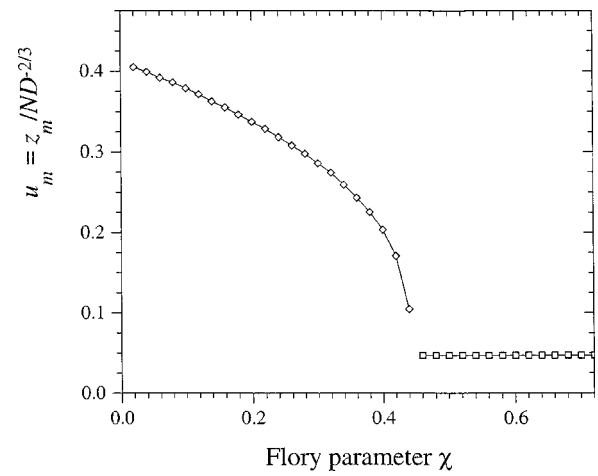


FIG. 13. The average reduced length $u_m = z_m/ND^{-2/3}$ as a function of the Flory interaction parameter χ , in the case $N=200$ and $D=5$. The horizontal line represents the value u_{\min} which would correspond to a completely collapsed chain.

behavior is the same as in Fig. 11. If both quantities $(m_{N,D}(u) - \langle m_{N,D} \rangle)/ND^{-5/3}$ and $(m_{N,D}(\rho) - \langle m_{N,D} \rangle)/ND^{-5/3}$ are plotted as a function of the reduced quantities u/u_m and ρ/ρ_m , respectively, both curves superpose quite exactly.

V. FREE ENERGY OF THE CONFINED CHAIN

A SAW of N steps, confined in a pore, is characterized by its length z (or r_{\parallel}) and the contact number m . Each contact is supposed to reduce the energy by an amount $k_B T \chi$, where χ is the Flory interaction parameter. From the joint probability distribution $P_{N,D}(z, m)$, which gives the number of configurations having m contacts and a length z , one can compute the z -partition function $Z_{N,D}(z, \chi)$, defined as

$$Z_{N,D}(z, \chi) = \sum_m P_{N,D}(z, m) e^{\chi m}. \quad (25)$$

The thermal and geometrical properties of the chain may be obtained from $Z_{N,D}(z, \chi)$. Then, from Eq. (25), a numerical model expression may be derived for the free energy of the chain, defined as $F_{N,D}(z, \chi) = -k_B T \ln Z_{N,D}(z, \chi)$. The average length z_m of the chain is then found by minimizing $F_{N,D}(z, \chi)$ for each value of χ . An example is shown in Fig. 13, in which the average reduced length $u_m = z_m/ND^{-2/3}$ is plotted as a function of the Flory parameter χ , in the case $N=200$, $D=5$. The horizontal line at high χ values (corresponding to bad solvent cases) represents the minimum value of u_m , which would correspond to the completely collapsed (dense) chain.

An analytic expression for $F_{N,D}(z, \chi)$ may be derived at small χ values. If $Z_{N,D}(z, \chi)$ is written formally as

$$Z_{N,D}(z, \chi) = \bar{P}_{N,D}(z) e^{\chi \bar{m}_{N,D}(z, \chi)}, \quad (26)$$

then $\bar{P}_{N,D}(z)$ and $e^{\chi \bar{m}_{N,D}(z, \chi)}$ are defined, respectively, as

$$\bar{P}_{N,D}(z) = \sum_m P_{N,D}(z, m), \quad (27)$$

$$e^{\chi \bar{m}_{N,D}(z,\chi)} = \frac{\sum_m P_{N,D}(z,m) e^{\chi m}}{\sum_m P_{N,D}(z,m)}. \quad (28)$$

Note that only in the limit $\chi \rightarrow 0$ may the contact number given by Eq. (19) be identified to $\bar{m}_{N,D}(z,\chi)$ defined in Eq. (28). Thus, using Eqs. (23) and (24), one gets the following model expression for $F_{N,D}(z,\chi)$ at small χ values, as a function of the reduced length $u = z/ND^{-2/3}$,

$$\frac{F_{N,D}(z,\chi)}{k_B T N D^{-5/3}} \cong (0.257 - 0.54\chi) u^{-5/4} + (4.03 + 3.6\chi) u^{5/2}. \quad (29)$$

Terms independent of u have been discarded, and only leading power terms have been retained. The right-hand side in Eq. (29) does *not* depend on the pore diameter D . Thus, the thermal behavior of the chain (i.e., the temperature at which the coil-globule transition occurs) is not affected by the confinement in the pore. Indeed, the model expression Eq. (29) has a scaling structure similar to that of a free SAW in three dimensions.¹² The main difference is the exponent $-5/4$ in the first term of the right-hand side, which describes the compact configurations of the chain.

VI. CONCLUSION

We have studied a polymer chain (a SAW) grafted at one end on a surface and confined in a pore, in the regime where the pore diameter is relatively small compared to the unperturbed size of the chain. The scaling of the radius of gyration along the tube as a function of both the chain length and the pore diameter, shows that a one-dimensional regime is established for a ratio R_F/D as low as 1.5. We have measured the probability distribution for the length of tube occu-

ried by the chain, on the one hand, and the number of contacts as a function of this length, on the other hand. Thus, we have been able to propose a numerical, model expression for the free energy of the grafted, confined chain as a function of the Flory interaction parameter χ . Discarding numerical coefficients, this model expression has a scaling form $F_{N,D}(z,\chi) \approx k_B T N D^{-5/3} ((1 - 2\chi) u^{-5/4} + (1 + \chi) u^{5/2})$, in which $u = zD^{2/3}/N$ is a reduced length of the chain. Thus, the thermal behavior is not affected by confinement in this model.

¹M. Daoud and P. G. de Gennes, *J. Phys. (France)* **38**, 85 (1977).

²P. G. de Gennes, *Scaling Concepts in Polymer Physics* (Cornell University Press, Ithaca, 1979).

³F. Brochard and P. G. de Gennes, *J. Phys. (France)* **40**, L-399 (1979).

⁴J. Lal, S. K. Sinha, and L. Auvray, *J. Phys. II* **7**, 1597 (1997).

⁵O. V. Borisov, T. M. Birshtein, and E. B. Zhulina, *J. Phys. II* **1**, 521 (1991).

⁶E. B. Zhulina, O. V. Borisov, and T. M. Birshtein, *J. Phys. II* **2**, 63 (1992).

⁷O. V. Borisov, E. B. Zhulina, and T. M. Birshtein, *Macromolecules* **27**, 4795 (1994).

⁸A. Chakrabarti and R. Toral, *Macromolecules* **23**, 2016 (1990).

⁹Pik-Yin and K. Binder, *J. Chem. Phys.* **95**, 9288 (1991).

¹⁰D. Lhuillier, *J. Phys. (France)* **49**, 705 (1988).

¹¹J. M. Victor and D. Lhuillier, *J. Chem. Phys.* **92**, 1362 (1990).

¹²J. M. Victor, J. B. Imbert, and D. Lhuillier, *J. Chem. Phys.* **100**, 5372 (1994).

¹³J. B. Imbert and J. M. Victor, *Mol. Simul.* **16**, 399 (1996).

¹⁴J. B. Imbert, A. Lesne, and J. M. Victor, *Phys. Rev. E* **56**, 5630 (1997).

¹⁵M. Bishop and C. J. Saltiel, *J. Chem. Phys.* **95**, 606 (1991).

¹⁶J. Reiter, T. Edling, and T. Pakula, *J. Chem. Phys.* **93**, 837 (1990).

¹⁷J. Reiter, *Macromolecules* **23**, 3811 (1990).

¹⁸M. T. Gurler, C. C. Crabb, D. M. Dahlin, and J. Kovac, *Macromolecules* **16**, 398 (1983).

¹⁹A. M. Ferrenberg and R. H. Swendsen, *Phys. Rev. Lett.* **61**, 2635 (1988).

²⁰J. B. Imbert, Ph.D. thesis, Université Paris VI, 1995.